Alexandria Engineering Journal (2018) 57, 35–47

HOSTED BY

Alexandria University

Alexandria Engineering Journal

www.elsevier.com/locate/aej
www.sciencedirect.com

ORIGINAL ARTICLE

Investigation of bending fatigue-life of aluminum sheets based on rolling direction

Raif Sakin

Department of Machine and Metal Technologies, Edremit Vocational School of Higher Education, Balıkesir University, 10300 Edremit, Balıkesir, Turkey

Received 28 March 2014; revised 29 March 2016; accepted 6 November 2016
Available online 24 November 2016

KEYWORDS

AA1100;
AA1050;
Aluminum sheet;
Bending fatigue life;
Rolling direction

Abstract High-cycle fatigue (HCF) and low-cycle fatigue (LCF) fatigue lives of rolled AA1100 and AA1050 aluminum sheets along different directions were evaluated at room temperature. Four types of samples denoted as longitudinal (L) and transverse (T) to the rolling direction were compared because the samples along the two typical directions show an obvious anisotropy. A cantilever plane-bending and multi-type fatigue testing machine was specially designed for this purpose. Deflection-controlled fatigue tests were conducted under fully reversed loading. The longest fatigue lives in the LCF region were obtained for AA1050 (L) while AA1100 (L) samples had the longest fatigue lives in the HCF region.

1. Introduction

Aluminum is a light material with a density (2.7 g/cm^3) that is approximately three times lower than the density of materials such as iron, copper, and brass. Aluminum shows perfect resistance to corrosion under various environmental conditions such as air, water, and sea, as well as under the action of different chemicals. Aluminum possesses attractive characteristics such as esthetic appearance, machinability, and high electric and heat conductivity. Aluminum is quite commonly used in the automotive industry and in aircraft owing to its physical, mechanical, and tribological characteristics [1–3]. Fatigue is an important parameter for determining the behavior of mechanical parts functioning under variable loads. The fatigue resistance of a structural component is affected by mechanical, metallurgical, and environmental variable factors. Fatigue is the primary reason for 80–90% of engineering failures. In applications that frequently use aluminum composites, determining the fatigue performance of the operating element and the effects of the operating parameters on fatigue is necessary. Fatigue assessment can be typically performed using the S-N (i.e. stress life) or the crack growth method [4]. Establishing extensive databases, including stress–life (S–N) information, is very important for precise evaluation of the fatigue characteristics of an element resulting from different operating conditions [1]. In engineering applications, relatively low-frequency strain cycling as a consequence, e.g., of start and stop operations, generates low-cycle fatigue (LCF) failure [5]. There are many crack origins due to high stresses that accompany LCF [6]. According to the literature [7], the fatigue properties of ultrafine-grained materials show an enhanced fatigue life under HCF. But, a limited number of studies were carried out on high cycle fatigue (HCF) and low cycle fatigue (LCF) of pure aluminum [7,8]. Fatigue life is particularly affected not only by

E-mail address: rsakin@balikesir.edu.tr
Peer review under responsibility of Faculty of Engineering, Alexandria University.

http://dx.doi.org/10.1016/j.aej.2016.11.005

Nomenclature

L	parallel (longitudinal) to the rolling direction	N_o	mean fatigue life
T	perpendicular (long-transverse) to the rolling direction	R_d	deflection rate
HCF	high cycle fatigue ($N_f > 10^5$)	R	stress rate
LCF	low cycle fatigue ($N_f < 10^5$)	R	reliability level
S_L	fatigue strength along longitudinal direction	R^2	correlation coefficient
S_T	fatigue strength along long-transverse direction	U_{min}	minimum deflection (negative value)
S_u	ultimate tensile strength	U_{max}	maximum deflection
N	number of cycles	S or σ	maximum stress amplitude
N_f	number of cycles to failure	a, b	constants of the material

the characteristics of a material but also by the characteristics of the relevant specimen: microcavities created when an aluminum part is produced, surface flaws, hot or cold deformation, and changes in the grain structure [9–14]. Tensile strength and fatigue life of aluminum were affected slightly by rolling direction at room temperature. However, when the ambient temperature increases, the tensile strength and fatigue life were significantly changed based on the rolling direction [12].

In their studies on some aluminum alloys, Srivatsan et al. have defined that yield, tensile and fatigue lives of the samples cut in the long-transverse (T) direction decrease in high test temperatures and high vibrational amplitudes in comparison with the samples cut in the longitudinal direction (L). However, at room temperature, the effect of the rolling direction on the yield, tensile and fatigue strength is not significant. The increase in temperature causes the decrease in tensile and fatigue strength by enlarging the grain structure [12,14]. In particular for the people working under different environmental conditions, the fatigue characteristics defined according to the rolling direction are of great importance. In general, the "stress amplitude-fatigue life curve" (S-N) of aluminum samples tested in both the longitudinal direction and the long-transverse direction indicates an increasing tendency for fatigue in response to the decreasing stress amplitude. Generally, by taking the testing time into consideration, values voluntarily cut in 10^6 cycles are used. However, in low stress amplitudes, the fatigue life of the material can be indefinite, because no fatigue failures occur reaching to 10^6 cycles.

In fact, apart from other metals, pure aluminum and its compounds are stated not to have a distinct fatigue strength limit. However, according to the usage areas and material characteristics (shape, size factor, etc.), there are surface centered cubic metals having well-defined fatigue limits [12]. In this study to better determine the fatigue strength limitations of AA1100 and AA1050 aluminum materials, the tests were continued up to 10^7 cycles. In the S-N curves, it is desirable to use the test data indicating the effects of the different stress rate (R) and mean stress values. However, because the test data for which the mean stress is zero and the fully reversed variable ($R = -1$) model is used are the most critical data, these values are used mostly in designing. Moreover, these data help the designer make quick and correct decisions about fatigue life [15–18]. AA1100 and AA1050 aluminum sheets are used particularly for plates and appliqués in the automobile industry, where high strength is not required but high ability for shaping and corrosion resistance is necessary. Chemicals and foods are carried in thin sheet metal vessels, in tubes and general containers manufactured by deep drawing and spinning processes, in heat exchangers, in welded assemblies, in vehicle plates, and in lighting such as light reflectors [3,19].

The main purpose of this study was to evaluate the effects of the rolling direction at room temperature on the AA1100 and AA1050 aluminum sheets used in the above-mentioned fields, evaluating the tensile characteristics and bending fatigue. In accordance with the aim of the study, a cantilever plane-bending and multiple-specimen test machine was specially designed and produced. In our study reported in the Ref. [10], because it was used for a single-specimen fatigue test device, the testing frequency was chosen as 70 Hz by taking the total test time into consideration. However, in this study, the testing device that we have recently designed that can be connected with four specimens at the same time performed the tests at a frequency of 50 Hz. At this high frequency and using the deflection-control fatigue test device, the fatigue tests of L and T specimens were performed on AA1100 and AA1050 aluminum sheets. According to the experimental results, S-N diagrams (Wöhler curves) were obtained. The stress corresponding to 10^7 cycles was considered as the fatigue life limit (endurance limit). The results were interpreted comparatively. In this study, the fatigue lives of commercial-purity aluminum sheets were considered based on two rolling directions (longitudinal and long-transverse).

2. Materials and method

2.1. Aluminum sheet specimens

In this study, aluminum sheets of commercial purity and cold-rolled products, with chemical content and standard presentations given in Table 1, were used. AA1100 and AA1050 aluminum sheets were supplied from the domestic market in Turkey. The test specimens were prepared by cutting into dimensions of 25 × 200 × 3 mm in parallel (longitudinal) and perpendicular (long-transverse) to the rolling direction (Fig. 1). These prepared aluminum specimens were subject to tensile and three-point bending tests according to TS-EN/485-2 and ISO 7438:2005(E). The test results are presented in Table 2 [20–23], and these results were observed to be consistent with the Refs. [3,10,22–25].

Table 1 Chemical composition of aluminum alloys (wt%).

Aluminum	Cr	Cu	Fe	Mg	Mn	Ni	Si	Ti	Zn	Al
AA1100	0.002	0.001	0.494	0.005	0.001	0.001	0.098	0.014	0.008	Bal.
AA1050	–	0.006	0.196	0.002	0.117	–	0.065	0.0157	0.004	Bal.

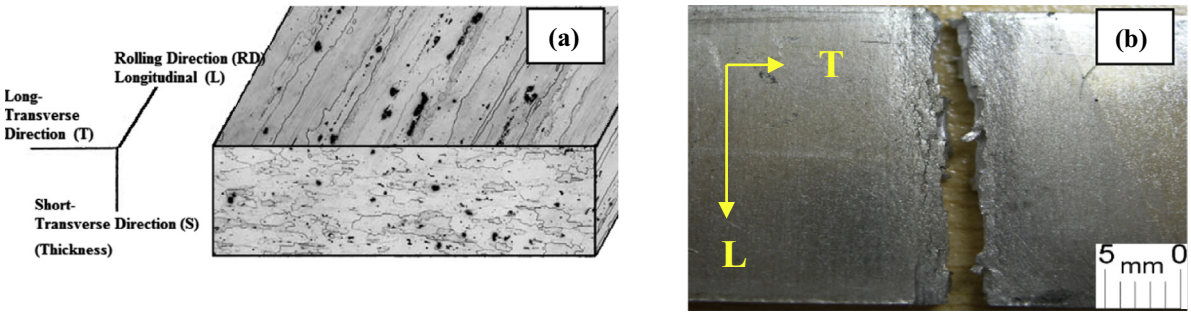

Figure 1 (a) Different orientation structures for specimens (L, T and S) and schematic micrograin structure; (b) broken AA1100 (T) aluminum specimen.

Table 2 Some mechanical characteristics of aluminum sheets [10,22,23,25,26].

Specimens and orientation	Tensile strength (MPa)	Yield strength (MPa)	Elastic modulus (GPa)	Bending strength (MPa)	Bending modulus (GPa)	Hardness (HB)
AA1100 (L)	126	120	69	120	60	32
AA1100 (T)	124	118	69	117	54	32
AA1050 (L)	117	106	69	106	54	30
AA1050 (T)	113	98	69	103	48	30

2.2. A cantilever plane bending and multiple specimen fatigue tests

In the closed-loop bending fatigue tests, the stress control or strain control can easily be used. In the stress-controlled test device, the test specimen is turned between the defined maximum-minimum loads, and the fixed stress amplitude is provided. As the fatigue process progresses, the strain increases and the rigidity decreases. As far as the strain-control is concerned, the specimen works between the defined maximum-minimum deflection, and the fixed strain amplitude is gained. Many commercial servo-hydraulic testing machines with stress control are significantly higher in complexity and in terms of maintenance, process and service costs as well as purchase costs compared to the strain-controlled testing device [27]. Thus, in this study, a cantilever-type plane bending fatigue testing device with deflection control, whose schematic picture is shown in Fig. 2, was designed and produced [22,23].

Maximum bending strength data obtained from the three-point bending tests were useful for determining the initial stress levels in the S-N curves [10,25,26,28–32]. All tests were performed at room temperature, and the stress ratio used was (fully reversed) $R = -1$. At least 200 materials were broken into pieces to obtain four specimen groups with two different orientation structures (L and T). Ten stress levels were determined to obtain the S–N curves corresponding to each group. On average, five specimens for each stress level were broken, meaning 50 specimens in total were tested. Bending fatigue tests were performed in the deflection-controlled cantilever-type device, which can be connected with four specimens at the same time, at a frequency of 50 Hz as shown in Figs. 2 and 3. The tests were continued up to 10^7 cycles [10,22,23,25,28,30,31].

2.2.1. Fatigue test device

In the fatigue test device, the motor used for the test was a 2.2 kW-2880 rpm motor. The motor with the V-belt started the main axle, and the testing frequency of ~50 Hz was obtained (Fig. 2). With the two holders on both sides of the pulley, the movement is distributed in two directions. Optionally, with a "separation arm", the movement of one side can be stopped, and the other side can continue (Fig. 3a). The main axles have a fixed 7.5 mm axis at the tip points. In response to the fixed amount of eccentricity, the binding parts of the specimens were made with sliding, so that the deflection can be changed according to the distance to the seat points (Figs. 2a and 3e). On the control panel, a "frequency adjuster" increases the motor frequency from 0 to 50 Hz. There is also an "emergency button" for emergency cases, a turn on/off button for electricity, and an "LCD monitor" to show the cycles of the specimens (Fig. 2a). A counter circuit was designed for general purposes. Counting circuit inputs work with a square wave of 12 volts coming directly from the specimen. In other words, the test specimens work as electric switch at the same time (Figs. 2a and 3d). As it can be seen in Fig. 2a, the proximity sensors on the mechanical contrivance are placed

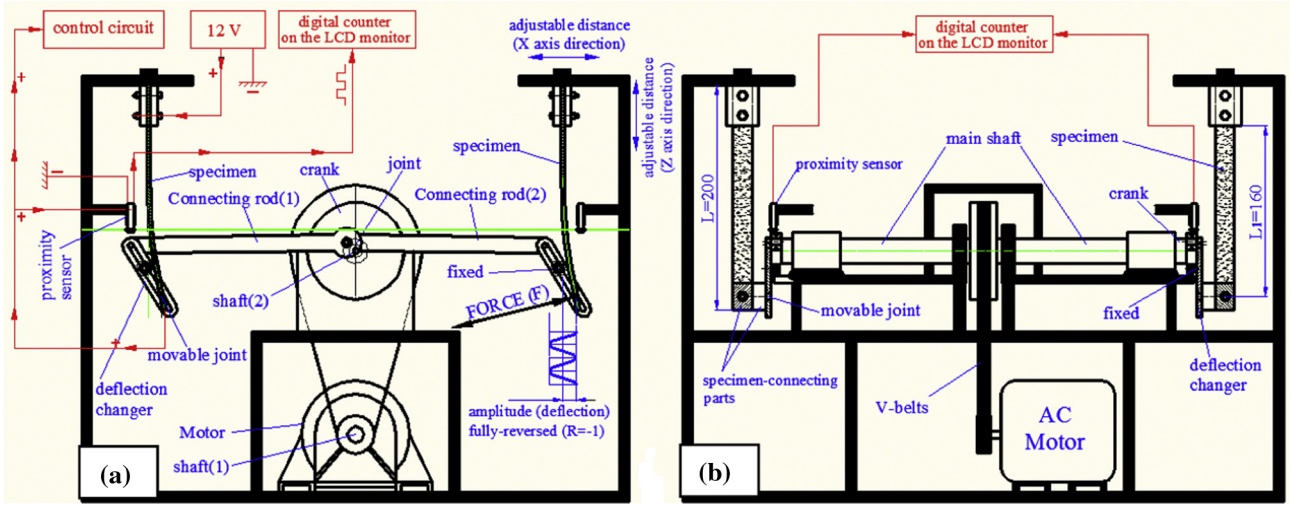

Figure 2 Schematic illustration of the cantilever plane-bending fatigue test machine: (a) side view and (b) front view.

capacitively in a manner to give "signals" when they see the metal piece in front of them [33]. Fixed deflections in the test were measured by a comparator with a resolution of 0.01, which was placed on the adjustment screws on the slide and on the specimen side (Fig. 3c).

Before starting the fatigue tests, to determine the required maximum force to be applied against each deflection value, the force-deflection tests that are shown in Fig. 3c were performed. In those tests, a FS800-type digital indicator of 5000 N capacity and an SS300-S type load cell of 0.5 N calibration sensation were used. To measure the deflection during the loading, a comparator was again used. In response to each deflection value for L and T specimens, the average force values measured by loadcell are close to each other; the difference between these values is negligible.

As it can be seen in Fig. 3d, the cantilever beam mechanism can be moved in x and z direction. Through this option, it can be tested under different deflection rates. When the specimen is broken, the signal is transmitted to the electro-mechanical puller and the specimen is pulled in the x-direction (Fig. 3d). This system prevents the friction between the fracture surfaces. An oscillating specimen holder is connected with hinge on the sliding system. Thanks to this system, bending force is always perpendicular to the plane tangent to the surface of the specimen (Fig. 3e).

In this study, deflection-controlled fatigue tests were carried out by using different deflections. To characterize the test, a deflection rate of $R_d = U_{\min}/U_{\max}$ was defined, similar to the stress rate ($R = \sigma_{\min}/\sigma_{\max}$). $U_{\min}$ and $U_{\max}$ are defined as deflection amplitudes. $U_{\min}$ is the minimum deflection (negative value), and $U_{\max}$ is the maximum deflection. These values are equal in absolute value to each other and are defined as $R_d = -1$. Mean stress is zero. The parameters of testing are shown in Table 3.

At the beginning of the fatigue test, the maximum force and initial deflection values to be applied to the specimens should be calculated. The deflection, bending force and stress values were calculated as *a cantilever beam loaded by a single force at its free end* [10,22,23,26]. Ten different deflection values were found by decreasing the initial deflection value at the rate of 20%. These values were first put in their places in the related equation to calculate the bending forces. These theoretical force calculations are close to the force value measured experimentally as shown in Fig. 3c; the differences are negligible. Then, the bending stress amplitude values (S) were calculated to compose S-N curves (Table 4). To obtain the S-N curves given in Fig. 4, five for each deflection (50 each for L and T directions), 200 specimens in total were broken. To evaluate the experimental data statistically and to find the average cycles to failure, the Weibull distribution of two parameters was used, and a regression analysis was used to obtain S-N curves [10,25,28,34–36]. All test results are presented in Table 4.

3. Testing results and discussion

3.1. S-N curves

Stress and average cycles to failure for each deflection value are given in Table 4, and the S-N curves obtained are shown comparatively in Fig. 4. To characterize the fatigue curves, the simplified Basquin exponential function is given in Eq. (1), and the function parameters gained are given in Fig. 4.

$$S = a(N_f)^{-b} \tag{1}$$

where

S: the stress amplitude or fatigue strength

N_f: the cycles to failure

a and b are the constants of the material (given in the equation in Fig. 4)

Empirical formulas indicating the relationship between the tensile strength of the aluminum specimens with rectangular sections in different cycles (S_u) and fatigue strengths depending on the specimen direction (S_L and S_T) are given in Table 5. The data obtained are in agreement with the literature [36].

3.2. Investigation of the fracture zone and surface

Depending on the direction of the bending (tension-compression) forces applied in opposite directions, fatigue

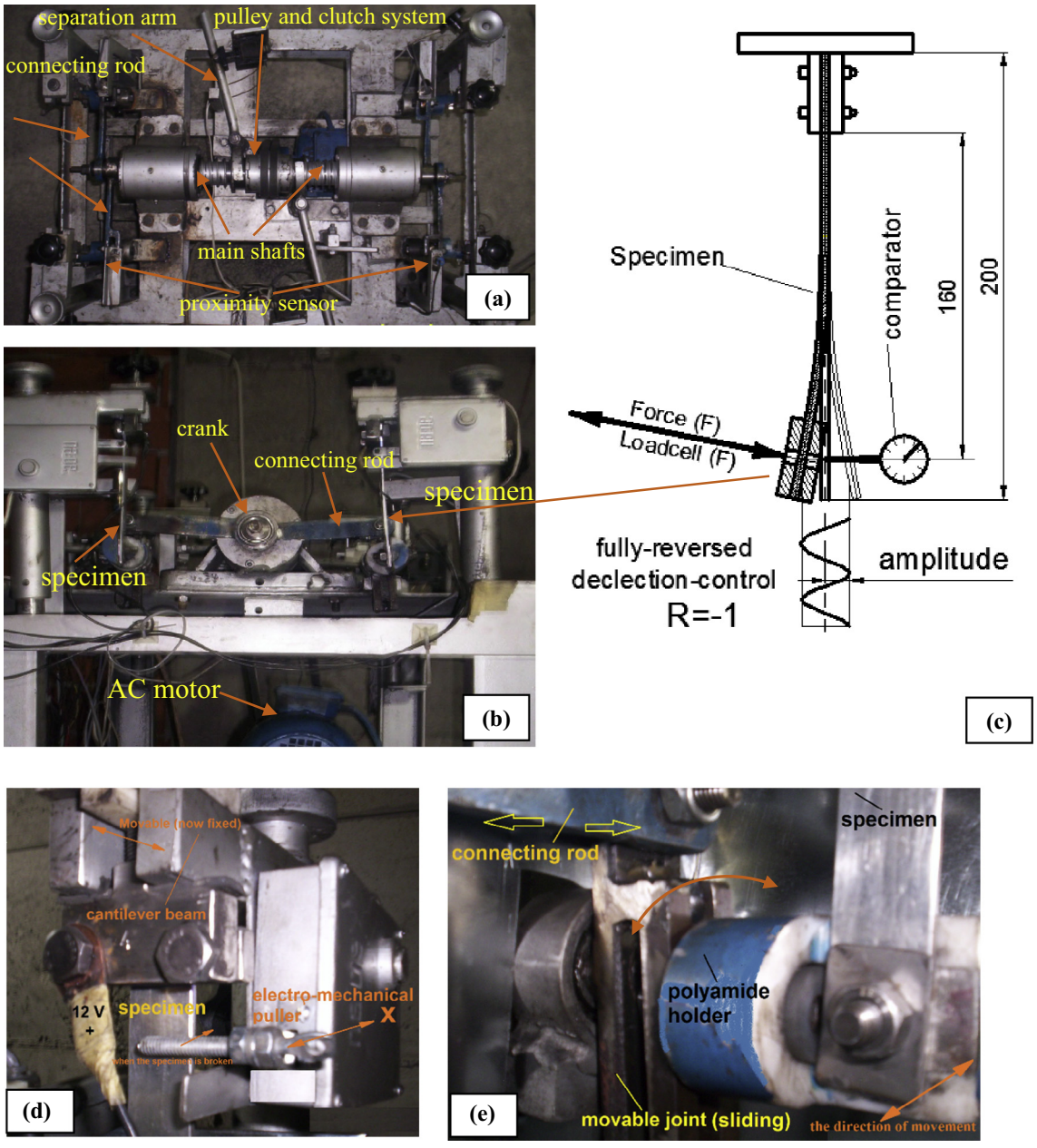

Figure 3 Photographs of the cantilever plane-bending fatigue test machine: (a) top view, (b) side view, (c) schematic force and deflection measurement, (d) the side of cantilever beam, and (e) moving side of the specimen.

Table 3 Test parameters.

Test frequency	50 Hz (adjustable from 0 to 50 Hz)
Temperature	Room temperature
Control	Deflection-controlled
Deflection rate	$R_d = -1$ (fully reversed)
Maximum cycle	10 million
Specimen preparation direction	Longitudinal direction (L)
	Transverse direction (T)

regions occurred from the top surface to the center of the cross section, and a suddenly fracture region occurred in the center of the cross section (Fig. 5). The sudden fracture always occurred in the middle area. This case is a significant indicator that the deflection rate is $R = -1$ (fully reversed) bending fatigue. In Fig. 6, the top surface view of an aluminum specimen tested in the T direction as a result of fracture is observed. The longitudinal long and deep macro cracks can easily be observed through visual inspection. As the cracks on the top surface of the specimens given in Figs. 6 and 7 are inspected, the cracks are observed to start on both sides of the broken area at more than one point, and the lateral cracks are sheer. Longitudinal cracks are parallel to the surface. As the local stress in the areas prone to the occurrence of cracks increased, the number of points where the cracks started also increased (Fig. 7). Cracks starting from more than one origin on the fracture surface are combined and then compose an unique

Table 4 S-N data of aluminum specimens.

Material	Deflection (mm)	Strength (MPa)	Test-1 (cycle)	Test-2 (cycle)	Test-3 (cycle)	Test-4 (cycle)	Test-5 (cycle)	Weibull parameters		Mean life (cycle)
								Alpha (α)	Beta (β)	
AA1100		126.00						1	1.00	1
(L)	10.00	105.47	996	998	1065	1068	1140	1083	17.02	1050
	8.00	84.38	1425	1452	1496	1502	1568	1515	27.34	1485
	6.40	67.50	1567	1603	1612	1638	1710	1652	29.76	1622
	5.12	54.00	2850	3603	3918	4100	4275	4016	6.25	3734
	4.00	42.19	6000	6112	6200	6413	8550	7227	5.35	6662
	3.20	33.75	61,988	63,035	64,118	64,125	64,126	63,964	63.65	63,399
	2.56	27.00	102,600	102,893	104,030	106,436	106,875	105,569	50.69	104,407
	2.00	21.09	192,375	509,634	512,487	513,000	525,825	546,672	1.92	484,977
	1.60	16.88	1,282,500	1,689,412	2,003,000	2,010,000	2,052,000	1,969,457	4.87	1,805,536
	1.30	13.71	9,634,008	10,260,000	10,562,000	10,773,000	12,436,750	11,226,467	10.11	10,685,087
AA1100		124.00						1	1.00	1
(T)	10.00	94.92	428	514	643	678	784	668	4.30	608
	8.00	75.94	784	1140	1148	1152	1283	1200	4.94	1101
	6.40	60.75	1636	1710	1753	1782	1782	1762	27.92	1728
	5.12	48.60	3398	3491	3633	3718	3848	3701	20.73	3606
	4.00	37.97	6038	7756	7908	7980	8550	8134	7.16	7618
	3.20	30.38	14,250	14,658	16,103	16,509	17,100	16,298	12.82	15,656
	2.56	24.30	10,006	26,719	27,075	27,888	36,985	30,773	1.88	27,317
	2.00	18.98	94,050	104,062	106,875	110,098	111,150	108,576	14.92	104,830
	1.60	15.19	1,682,571	1,689,412	1,702,659	1,710,000	1,795,500	1,742,086	31.98	1,712,282
	1.30	12.34	7,965,312	8,721,000	9,112,841	9,205,678	9,234,000	9,115,186	15.69	8,814,385
AA1050		117.00						1	1.00	1
(L)	10.00	94.92	1645	1998	2077	2222	2390	2196	9.03	2080
	8.00	75.94	3466	4620	5528	6491	7486	6145	3.46	5525
	6.40	60.75	8039	8811	9853	10,427	10,649	10,056	8.11	9476
	5.12	48.60	12,497	12,619	13,489	14,040	16,390	14,342	6.23	13,333
	4.00	37.97	27,171	29,164	30,476	30,833	32,049	30,815	18.26	29,928
	3.20	30.38	42,723	44,257	44,647	44,880	48,593	45,951	14.12	44,287
	2.56	24.30	94,350	99,368	102,337	104,114	106,068	103,422	25.82	101,258
	2.00	18.98	465,478	498,861	500,487	545,784	591,676	540,583	8.35	510,131
	1.60	15.19	1,280,176	1,403,949	1,968,412	2,005,168	2,125,308	1,919,493	3.38	1,723,861
	1.30	12.34	7,261,948	9,845,908	10,360,059	10,662,578	10,873,874	10,505,159	16.35	10,171,184
AA1050		113.00						1	1.00	1
(T)	10.00	84.38	1108	1652	1963	2274	2274	2079	4.45	1896
	8.00	67.50	3070	4045	6057	6082	7052	5946	2.76	5292
	6.40	54.00	9563	11,213	12,589	13,120	13,165	12,669	8.70	11,979
	5.12	43.20	14,111	14,765	15,677	18,244	18,765	17,119	5.96	15,876
	4.00	33.75	23,278	24,180	27,151	31,322	31,395	28,980	5.43	26,733
	3.20	27.00	32,174	32,205	34,668	36,344	41,044	36,549	6.95	34,178
	2.56	21.60	51,280	62,896	73,159	76,977	79,211	74,116	6.59	69,113
	2.00	16.88	254,786	304,423	314,134	455,301	515,933	405,690	2.56	360,194
	1.60	13.50	1,186,864	1,304,576	1,589,473	1,667,932	1,836,201	1,627,214	4.85	1,491,468
	1.30	10.97	3,328,553	6,968,361	9,382,195	10,489,276	10,624,187	9,575,582	3.35	8,596,266

crack zone. As observed in Figs. 8 and 9, because these cracks progressed on different planes, they split from each other with stair lines [22,37]. However, as the deflection value decreased and reached higher cycles, the stair lines decreased in size and became invisible (Figs. 8c and d, 9c and d). As observed in Figs. 6 and 8d, in T specimens, the crack progressed more easily between the grains. Instead of little cracks, a large crack progressed longitudinally between grains and caused fracture. In L specimens, smaller but more cracks were observed and as a result of the lateral progress of these small cracks, fracture occurred. As observed in Fig. 7, when the surfaces of the specimens were tested at the highest deflection value (10 mm), many lateral cracks progressing from the surface to the center were observed on the L specimens. This interpretation may mean that many cracks progressing from surface to center should occur for L specimens to break as a result of fatigue (Fig. 7a). As far as the T specimens are concerned, as observed in Figs. 6 and 7b, fracture generally occurred as a result of a few critical cracks starting from the surface and macro-size cracks that progress more rapidly and are a result of the union of these critical cracks. As the deflection value decreases and the cycle increases, lateral cracks become smaller. As far as the HCF ($N_f > 10^6$) region (deflection = 1.3 mm) is concerned, lateral cracks can be clearly distinguished in the L spec-

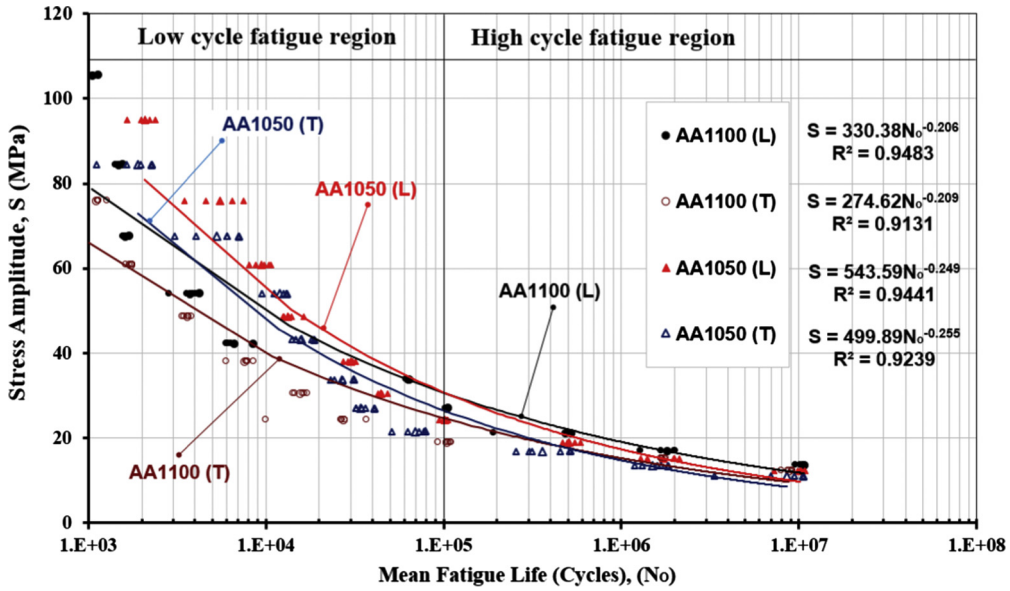

Figure 4 S-N curves for L and T directions.

Table 5 The relationship between tensile and fatigue strengths in response to some cycle values.

Specimens and orientation	Cycles to failure (N_f)				
	10^3	10^4	10^5	10^6	10^7
AA1100 (L)	$S_L = 0.63S_u$	$S_L = 0.39S_u$	$S_L = 0.24S_u$	$S_L = 0.15S_u$	$S_L = 0.09S_u$
AA1100 (T)	$S_T = 0.52S_u$	$S_T = 0.32S_u$	$S_T = 0.20S_u$	$S_T = 0.12S_u$	$S_T = 0.08S_u$
AA1050 (L)	$S_L = 0.84S_u$	$S_L = 0.47S_u$	$S_L = 0.26S_u$	$S_L = 0.15S_u$	$S_L = 0.08S_u$
AA1050 (T)	$S_T = 0.76S_u$	$S_T = 0.42S_u$	$S_T = 0.23S_u$	$S_T = 0.13S_u$	$S_T = 0.07S_u$

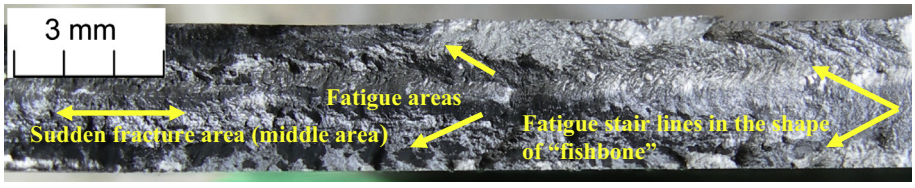

Figure 5 Optical view of the fracture surface in the direction of the cross section of the AA1100 (T) specimen.

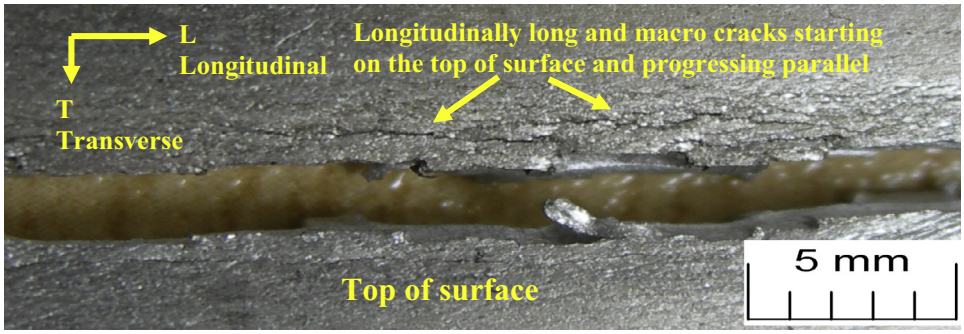

Figure 6 Macro cracks progressing on the top of the surface of the AA1100 (T) specimen.

imens, and lengthwise cracks can be distinguished on the T specimens. The stair lines in the shape of a "fishbone" (≪) that are observed on the surface of the fatigue fracture of AA1100 and AA1050 sheets, as in Figs. 5 and 8a, signify that fatigue cracks can progress on leaned planes as well [37,38].

As observed in Fig. 9a and b, there are hundreds of "thin fatigue lines" between "fishbone" signs. Many thin cracks or

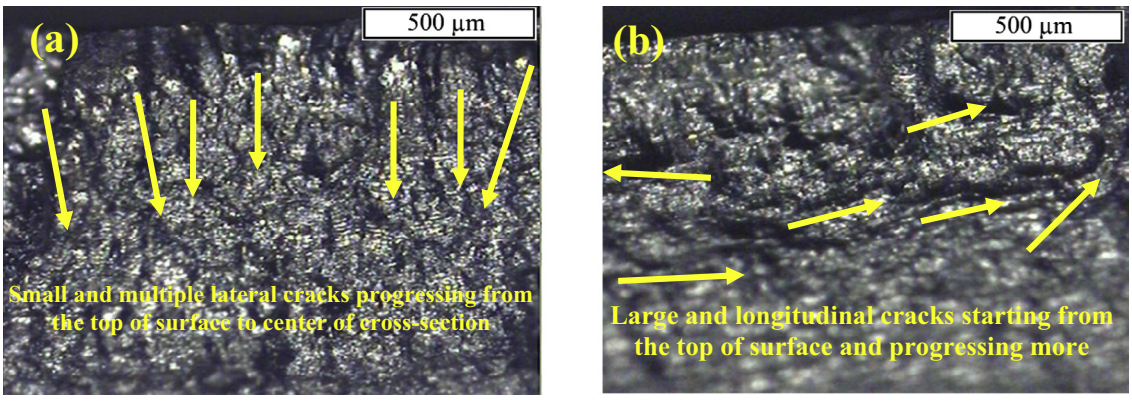

Figure 7 (a) Cracks starting from the top of the surface and progressing in the direction of main stress in the AA1100 (L) specimen. (b) Macro cracks starting on the top of the surface and progressing in a lateral (parallel) way in the AA1100 (T) specimen (deflection = 10 mm).

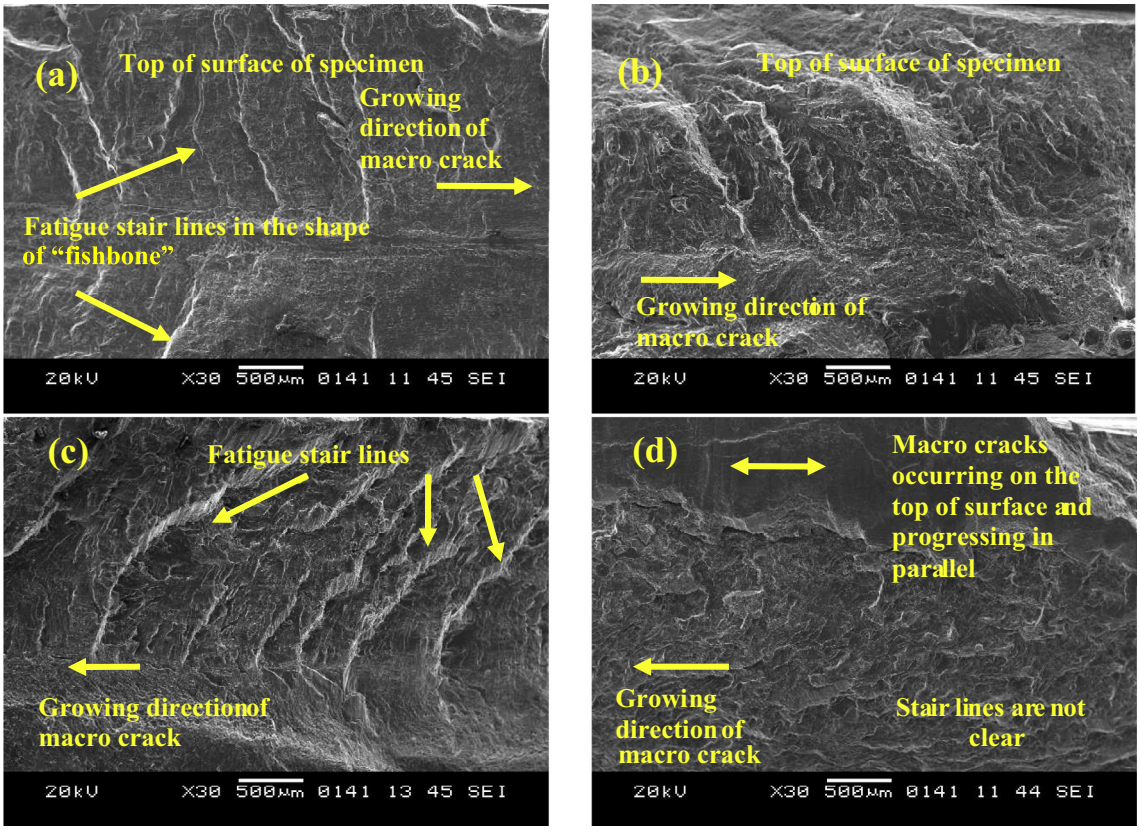

Figure 8 SEM view of the fracture surfaces: (a) AA1050 (L) specimen, fracture = 27,171 cycles; (b) AA1050 (L) specimen, fracture = 7,261,948 cycles; (c) AA1050 (T) specimen, fracture = 34,668 cycles; (d) AA1050 (T) specimen, fracture = 5,038,254 cycles.

tears are observed in these thin fatigue lines. The SEM view of the specimens in the HCF region is observed in Fig. 9c and d. Fatigue lines became thinner and denser in this area. In HCF tests of specimens having different orientation (L and T) structures, fatigue lines are observed to decrease, and the microstructure is similar. Thus, there is a slow and constant crack growing in high cycles close to 10^7 values. This case is a proof showing that the effect of the rolling direction in the HCF region on fatigue strength is less than the effect of the rolling direction in the LCF region. As observed in Fig. 4, going from the LCF region to the HCF ($N_f > 10^6$) region, the curves become closer to each other. Even in the S-N curves of aluminum sheets having a reliability level of $R = 0.99$ (99%), the effect of rolling direction on fatigue strength is observed to be only slightly less [10].

3.3. Factors affecting fatigue strength

Fatigue strength is affected by many factors such as testing frequency, specimen size (size effect), specimen geometry

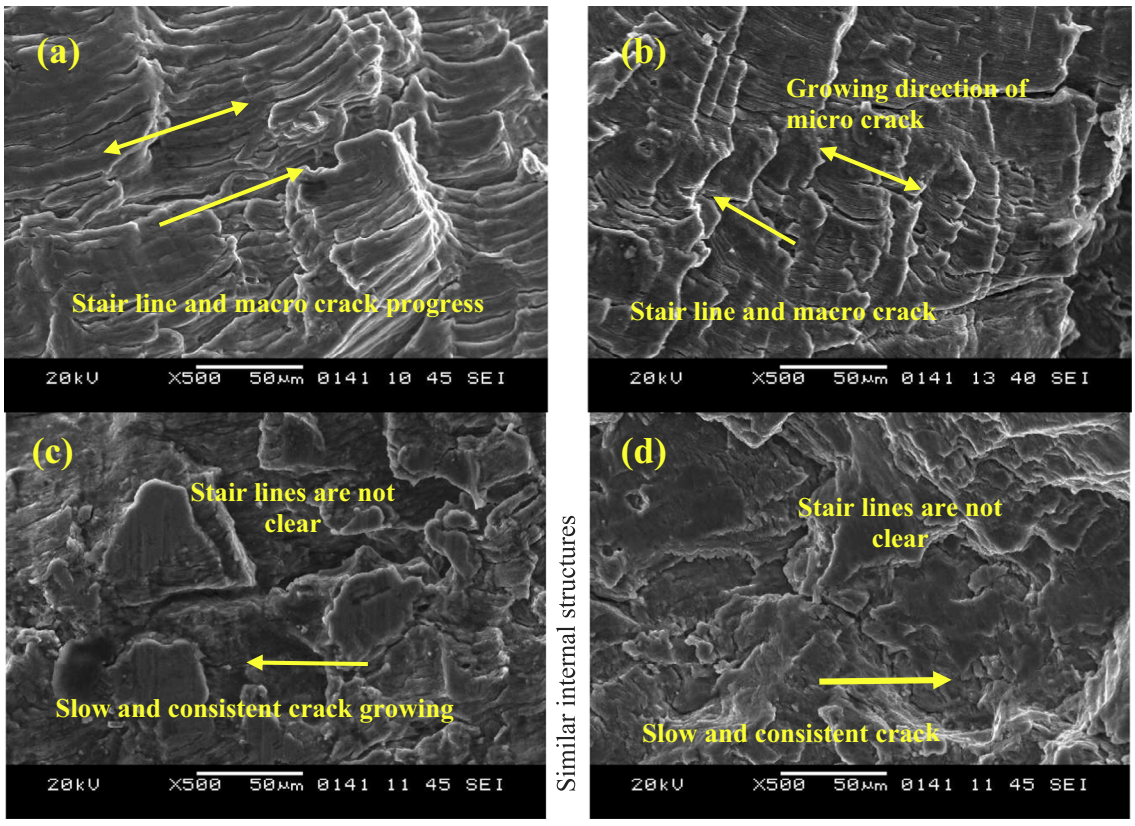

Figure 9 SEM view of fracture surfaces: (a) AA1050 (L) specimen, fracture = 27,171 cycles; (b) AA1050 (T) specimen, fracture = 34,668 cycles; (c) AA1050 (L) specimen, fracture = 7,261,948 cycles; (d) AA1050 (T) specimen, fracture = 5,038,254 cycles.

(geometrical effect), testing method, microstructure of the specimen and grain size. The details of these effects and mechanical characteristics of some commercial aluminum are given in the references [3,24,39–43].

3.3.1. Microstructure and the effect of grain size

If the processed aluminum alloys such as rolling or extrusions are exposed to repeated loadings, plastic deformation areas occur in fatigue areas. Plastic deformation depends on the grain size, grain structure, grain direction/non-direction, grain distribution, and grain morphology in this area of the specimen [44]. Cracks start primarily in the grain borders. In the area between grains, surface cracks are observed. As a result of the rolling and extrusion applications on materials, the presence of large grains in the micro structure and the characteristics of the grain borders accelerate the crack among the grains [45]. Grain size does not significantly affect the fatigue or tensile behavior in mass-centered and surface-centered metals having a traditional grain structure. However, grain size may be of little or much effect on the fatigue life of the surface-centered metals such as aluminum, copper, and α-brass [8]. Grain size has an important effect on fatigue life, especially in aluminum alloys [46]; especially in aluminum alloys, grain size and grain direction play a very significant role in deciding the fatigue life. The presence of lengthened grains with the sequence of other compounds, apart from aluminum, in the grain border affects fatigue life. With the decrease in stress level, the difference of fatigue strength between two directions (L and T) can increase. In other words, the decrease in the density of the other compound apart from aluminum significantly improves the fatigue strength at lower stress levels by bringing fatigue strength gained in both directions (L and T) closer [47]. Therefore, this characteristic is more apparent in commercially pure aluminum. There is a more ductile structure in the high stress and low cycle fatigue (LCF) region of aluminum and aluminum alloys due to the large grain structure (according to the HCF region). In the LCF region, due to the excessive sensitivity regarding ductile structure and shape change, tear bands occur in the macro size. Due to the repeated deformation under low stress in the HCF region, grains change shape, and a harder structure is formed [48]. Therefore, due to this structure change in the HCF region, the fatigue limits in the L and T directions are closer to each other. As the specimen is exposed to high stress amplitudes, a crack can start from a different position and then go on to the shear force direction (Figs. 6 and 7). As observed in Figs. 8 and 9, if the specimen is exposed to a lower tensile amplitude, the crack starts from a point and continues consistently [49].

In this study, to understand the fracture mechanisms in the LCF and HCF regions of L and T specimens, microphotographs of the fracture areas were taken before and after the tests, and these photographs are shown in Fig. 10. Internal structure and porosity of the fracture areas in $N \sim 10^7$ cycles of L and T specimens are very similar. As observed in Fig. 10(c), (d), (g), (h), grain borders, grain size, orientation, and grain structure are directed toward 45° planes. Therefore, cracks

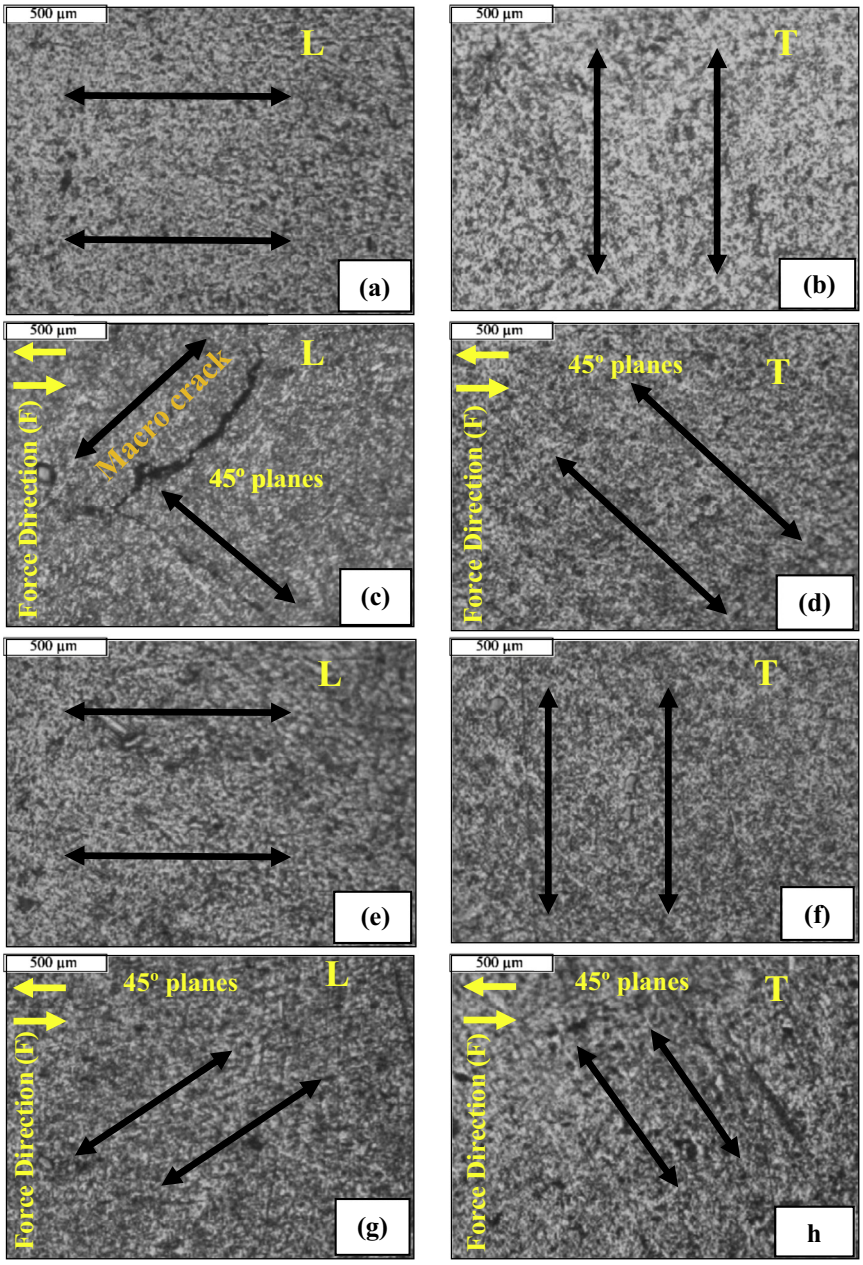

Figure 10 Microphotographs of the fracture areas in the direction of length and thickness for the AA1050 specimen, fracture for L = 1,403,949 cycles, deflection = 1.6 mm, fracture for T = 3,328,553 cycles, deflection = 1.3 mm, (a) and (b) vertical position, pre-test; (c) and (d) vertical position, post-test; (e) and (f) linear position, pre-test; and (g) and (h) linear position, post-test.

causing fracture toward both L and T directions are directed toward 45° planes. This case can be indicative that fatigue strength in L and T directions especially in the HCF region are at the same level. In other words, consistent deformation occurring in the aluminum sheets tested in the HCF region caused a very similar fracture mechanism on both sides by affecting the grain structure and grain borders. As mentioned above and in the references [22,23,47], because AA1100 and AA1050 are commercial aluminum sheets of high purity, they contain other compounds in small amounts. This case can be a proof for the improvement of similar fracture mechanisms for both directions.

3.4. Reliability levels of aluminum sheets at different cycles

In the calculation of the average fatigue life, a Weibull distribution was used, and α, β parameters characterizing this distribution were calculated [10,25,28,34,35]. Test results and the Weibull parameters (α and β) calculated for each stress level and estimated mean life values are given in Table 2. Graphics of "*reliability or probability of survival*" of the aluminum sheets in this study in both low cycle regions (LCFs) as 10^4–10^5 and high cycle regions (HCFs) are observed in Fig. 11. The most important characteristics of these graphics shown in Fig. 11 are that they facilitate the selection of the material. As the

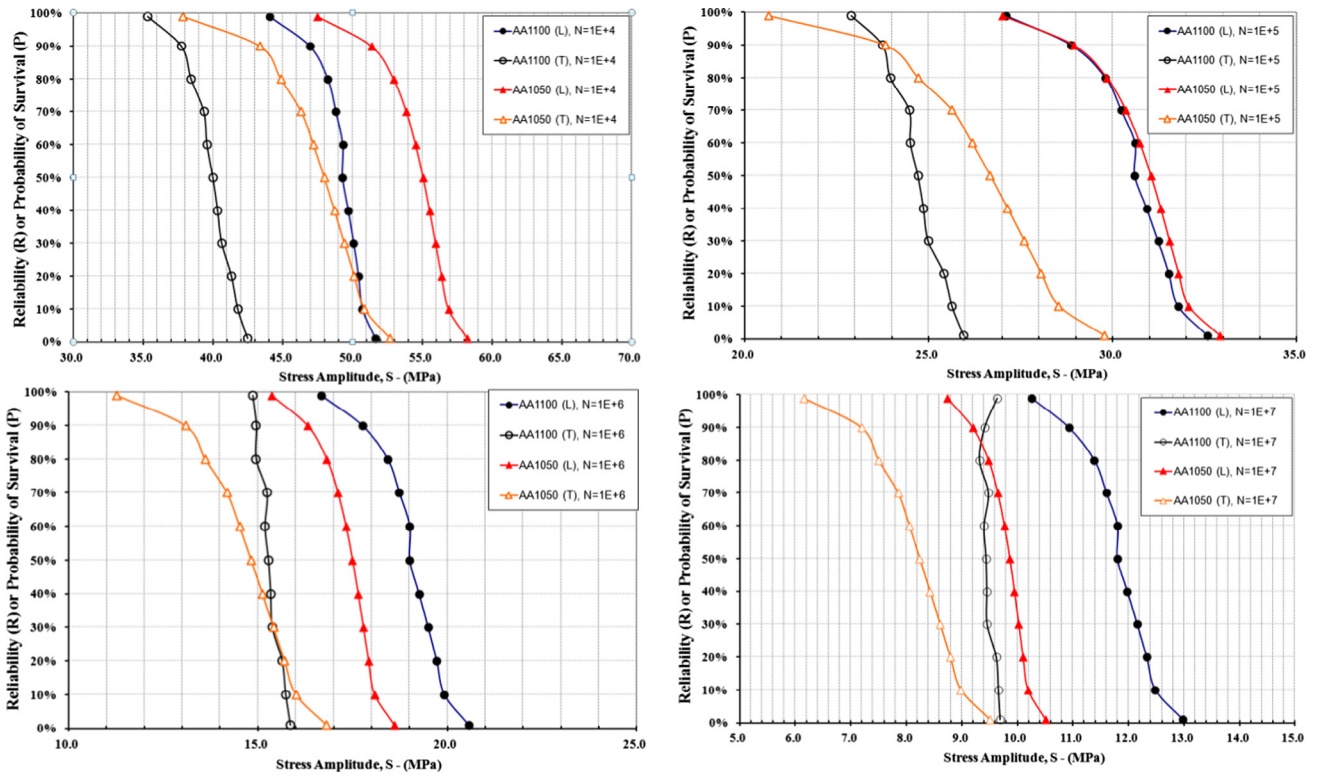

Figure 11 Reliability (Probability of Survival) graphs for low-cycle (LCF) and high-cycle fatigue (HCF) regions.

graphics of $N = 10^4$ and $N = 10^5$ cycles are concerned (Fig. 11a and b), in this low cycle region, AA1050 (L) should be chosen. In the high cycle regions (HCFs) of $N = 10^6$ and $N = 10^7$ cycles, AA1100 (L) should be preferred. Another example is that in the high cycle region of $N = 10^6$ cycles (Fig. 11c), our preference in the $R = 0.50$ (50%) reliability level between AA1100 (T) and AA1050 (T) should be AA1100 (T). From these diagrams, it is easy to find and compare the response, reliability percentage and fatigue life in response to any reliability value. In addition, reliability graphics are helpful to the designer in terms of material selection.

4. Conclusion

In this experimental study, the following results were obtained regarding the cantilever plane-bending fatigue behaviors of AA1100 and AA1050 aluminum sheets.

- According to the test results, although the tensile and yield values are a little higher in specimen cut in longitudinal direction (L), tensile characteristics are generally not much affected (1.6–3.4%) by the rolling direction at room temperature.
- In all aluminum sheets, as the cycles increase, fatigue strength eventually decreases. S-N curves at $R \approx 0.50$ (mean fatigue life) reliability level for all specimens were plotted, and power function parameters (a and b) were obtained. By using these curves, it is possible to estimate the fatigue life of related aluminum sheets under any stress. These curves provide the reliable fatigue lives required by the designer.
- The empirical formula indicating the relationship between tensile and fatigue strength for AA1100 and AA1050 with rectangular sections in different cycles are gained, which can lead designers in practical applications as well.
- Because AA1100 and AA1050 were commercial aluminum sheets of high purity (Al > 99%) and the tests were performed at room temperature, microstructure and grain size did not affect test results significantly.
- Because the internal structure and porosity in both rolling directions (L and T) are very similar and due to the consistent deformation in the HCF region, grain structure and grain borders were affected and similar fracture mechanisms occurred in both directions. Therefore, in the HCF ($N > 10^6$) region the effect of rolling direction on fatigue strength is less compared to the effect of rolling direction on fatigue strength in the LCF region.
- The effect of rolling direction on fatigue strength in the high-cycle fatigue (HCF) region is less than the effect of rolling direction in the low-cycle fatigue (LCF) region.
- As observed in S-N curves and reliability graphs, for the same reliability levels, the longest fatigue life in the LCF region between $N = 10^4$ and $N = 10^5$ cycles was gained in AA1050 (L), and the shortest fatigue life was gained in AA1100 (T) specimens. However, in the HCF region between $N = 10^6$ and $N = 10^7$ cycles, the longest fatigue life was gained in AA1100 (L), and the shortest fatigue life was gained in AA1050 (T) specimens.
- According to the test results, AA1100 and AA1050 aluminum sheets should be used in the places where high fatigue level and fatigue strength are not needed. In other words, it is more appropriate to make secure designs of this type of aluminum sheets to work dynamically in LCF region.

Acknowledgments

Some parts of this study were supported by the Scientific Research Projects Fund of 'Balıkesir University' and 'Celal Bayar University'. In addition, some of the tests regarding aluminum were conducted by using the facilities of the Ground Forces Sergeant Vocational School of Higher Education. The author therefore thanks Prof. Dr. İrfan Ay, Asst. Prof. Dr. Nurcan Kumru, Teacher-Squadron Leader Muharrem Er, the Seas Mechanic Company, and the Ground Forces Sergeant Vocational School of Higher Education for their support as well.

References

[1] R. Sadeler, Y. Totik, M. Gavgalı, I. Kaymaz, Improvements of fatigue behaviour in 2014 Al alloy by solution heat treating and age-hardening, Mater. Des. 25 (2004) 439–445.
[2] W.F. Smith, Materials Science and Engineering, Translated Author: Kınıkoğlu, N.G. (Turkish), Literature Publications, Istanbul, Turkey, 2001.
[3] E.L. Rooy, ASM International Handbook, Properties and Selection: Nonferrous Alloys and Special-Purpose Materials. In Introduction to Aluminum and Aluminum Alloys,, vol. 2, The Materials Information Company, USA, 2005.
[4] M. Soliman, G. Barone, D.M. Frangopol, Fatigue reliability and service life prediction of aluminum naval ship details based on monitoring data, Struct. Health Mon. 14 (2014) 3–19.
[5] Y.B. Unigovski, A. Grinberg, E. Gerafi, E.M. Gutman, Low-cycle fatigue of a multi-layered aluminum sheet alloy, Surf. Coat. Technol. 232 (2013) 695–702.
[6] A.N. Abood, A.H. Saleh, Z.W. Abdullah, Effect of heat treatment on strain life of aluminum alloy AA 6061, J. Mater. Sci. Res. 2 (2013).
[7] M.S. Soliman, E.A. El-Danaf, A.A. Almajid, Enhancement of static and fatigue strength of 1050 Al processed by equal-channel angular pressing using two routes, Mater. Sci. Eng., A 532 (2012) 120–129.
[8] H. Mughrabi, H.W. Höppel, Cyclic deformation and fatigue properties of very fine-grained metals and alloys, Int. J. Fatigue 32 (2010) 1413–1427.
[9] M. Değer, Effect of microstructure surface processes of fatigue strength of pearlitic-ferritic and pearlitic ductile cast irons, in: Institute of Science, Mechanical Engineering, Volume Ph.D. Thesis, Selcuk University, Konya, 1995.
[10] R. Sakin, M. Er, Investigation of plane-bending fatigue behavior of 1100–H14 aluminum alloy, J. Fac. Eng. Archit. Gazi Univ. 25 (2010) 213–223.
[11] T.S. Srivatsan, An investigation of the cyclic fatigue and fracture behavior of aluminum alloy 7055, Mater. Des. 23 (2002) 141–151.
[12] T.S. Srivatsan, Mechanisms governing cyclic deformation and failure during elevated temperature fatigue of aluminum alloy 7055, Int. J. Fatigue 21 (1999) 557–569.
[13] T.S. Srivatsan, S. Anand, S. Sriram, V.K. Vasudevan, The high-cycle fatigue and fracture behavior of aluminum alloy 7055, Mater. Sci. Eng., A 281 (2000) 292–304.
[14] T.S. Srivatsan, D. Kolar, P. Magnusen, The cyclic fatigue and final fracture behavior of aluminum alloy 2524, Mater. Des. 23 (2002) 129–139.
[15] T. George, Development of a novel vibration-based fatigue testing methodology, Int. J. Fatigue 26 (2004) 477–486.
[16] H.J. Sutherland, On the Fatigue Analysis of Wind Turbines, Sandia National Laboratories, Albuquerque, New Mexico, A.B. D., 1999.
[17] E. Ünal, Simulation of Fatigue Behaviour of E-Glass Fiber Reinforced Polyester Composites in atmospheric and Marine Environments, Institute of Science, Volume M.Sc., Ege University, Izmir, 2006.
[18] P.K. Mallick, Composites Engineering Handbook, CRC Press, New York, USA, 1997.
[19] H.K. Zeytin, T. Bilal, O. Arısoy, Aluminium Alloys, Applications, and Future of the Automotive Industry. In Project No: 50H5602, TUBITAK Marmara Research Center, Gebze, Turkey, 2000.
[20] TSE, TS EN 485-2: Aluminium and Aluminium Alloys Sheet Strip and Plate Part 2: Mechanical Properties, Turkish Standards Institute (TS), Ankara, Turkey, 2010.
[21] ISO, EN ISO 7438:2005(E), Metallic Materials, Bend test. Geneva, Switzerland, 2005.
[22] M. Er, Investigation of bending fatigue behaviour of the 1100–H14 aluminium plate and the design of a amplitude-regulated, high frequency bending fatigue test machine, in: Institute of Science, Department of Mechanical Engineering, Balıkesir University, Balikesir, Turkey, 2006.
[23] N. Kumru, Design of fatigue test apparatus for etial-141, etial-145 and etial-160 type cast aluminum and plate aluminum materials and investigation of bending fatigue behaviours, in: Institute of Science, Department of Mechanical Engineering, Celal Bayar University, Manisa, Turkey, 2007.
[24] M.L. Weaver, M.E. Stevenson, ASM international handbook, mechanical testing and evaluation, in: Introduction to the Mechanical Behavior of Nonmetallic Materials, vol. 8, Materials Information Company, USA, 2000.
[25] R. Sakin, N. Kumru, M. Er, I. Ay, Statistical analysis of fatigue-life data for aluminum alloys and composites, in: A. Oral (Ed.), 2nd National Congress of Design, Manufacturing and Analysis, Balikesir, Turkey, 2010.
[26] I. Ay, R. Sakin, Production and testing of glass-fiber reinforced plastic axial fan blades for replacement for aluminum ones that are produced in Balikesir, in: Scientific Research Project, Volume 2002/14. Balikesir University Research Foundation, Balikesir, Turkey, 2006.
[27] W.V. Paepegem, J. Degrieck, Experimental set-up for and numerical modelling of bending fatigue experiments on plain woven glass/epoxy composites, Compos. Struct. 51 (2001) 1–8.
[28] R. Sakin, İ. Ay, Statistical analysis of bending fatigue life data using Weibull distribution in glass-fiber reinforced polyester composites, Mater. Des. 29 (2008) 1170–1181.
[29] R. Sakin, İ. Ay, R. Yaman, An investigation of bending fatigue behavior for glass-fiber reinforced polyester composite materials, Mater. Des. 29 (2008) 212–217.
[30] İ. Ay, R. Sakin, G. Okoldan, An improved design of apparatus for multi-specimen bending fatigue and fatigue behaviour for laminated composites, Mater. Des. 29 (2008) 397–402.
[31] R. Sakin, N. Kumru, İ. Ay, Design of apparatus for the stress-controlled, multi-specimen bending fatigue test and an application for composites, in: C. Meran (Ed.), 12th International Materials Symposium (IMSP'2008), Volume 531–541, Pamukkale University, Denizli, Turkey, 2008, pp. 531–541.
[32] H.Y. Kim, T.R. Marrero, H.K. Yasuda, O.A. Pringle, A simple multi-specimen apparatus for fixed stress fatigue testing, J. Biomed. Mater. Res. 48 (1999) 297–300.
[33] N. Kumru, I. Ay, The design of new fatigue machine, which has multi-specimen and applying tension-compression stress for the determination of the bending fatigue strength of aluminum fan blades, Celal Bayar University, J. Tech. Sci. Soma Vocat. School 2 (2010) 41–55.
[34] S. Mohd, Y. Mutoh, Y. Otsuka, Y. Miyashita, T. Koike, T. Suzuki, Scatter analysis of fatigue life and pore size data of die-cast AM60B magnesium alloy, Eng. Fail. Anal. 22 (2012) 64–72.

[35] M. Sivapragash, P.R. Lakshminarayanan, R. Karthikeyan, K. Raghukandan, M. Hanumantha, Fatigue life prediction of ZE41A magnesium alloy using Weibull distribution, Mater. Des. 29 (2008) 1549–1553.
[36] P.S. Effertz, V. Infante, L. Quintino, U. Suhuddin, S. Hanke, J. F. dos Santos, Fatigue life assessment of friction spot welded 7050-T76 aluminium alloy using Weibull distribution, Int. J. Fatigue 87 (2016) 381–390.
[37] I.B. Eryürek, Failure Analysis, vol. 75–79, Birsen Publishing, Istanbul, Turkey, 1993.
[38] C. Glancey, R. Stephens, Fatigue crack growth and life predictions under variable amplitude loading for a cast and wrought aluminum alloy, Int. J. Fatigue 28 (2006) 53–60.
[39] E.S. Kayalı, C. Ensari, E. Dikeç, Mechanical Testing of Metallic Materials, Istanbul Technical University (ITU) Publications, Istanbul, 1983.
[40] E. Donnelly, D. Nelson, A study of small crack growth in aluminum alloy 7075-T6, Int. J. Fatigue 24 (2002) 1175–1189.
[41] T. Hassan, Z. Liu, On the difference of fatigue strengths from rotating bending, four-point bending, and cantilever bending tests, Int. J. Press. Vessels Pip. 78 (2001) 19–30.
[42] G. Murugan, K. Raghukandan, U.T.S. Pillai, B.C. Pai, Influence of transverse load on the high cycle fatigue behaviour of low pressure cast AZ91 magnesium alloy, Mater. Des. 30 (2009) 4211–4217.
[43] A.R.C. Markl, Fatigue tests of piping components, Trans. ASME 74 (1952) 287–303.
[44] S. Yip (Ed.), Handbook of Materials Modeling, Springer, Netherlands, 2005.
[45] J.A. VanDenAvyle, H.J. Sutherland, Fatigue characterization of a VAWT blade material, in: D.E. Berg, P.C. Klimas (Eds.), Eighth ASME Wind Energy Symposium, vol. 7, ASME, 1989, pp. 125–129.
[46] C.H. Gür, J. Pan, Handbook of Thermal Process Modeling of Steels, USA, 2009.
[47] M.A. Malik, S. Iftikharus, W. Muhammad, N. Ejaz, Effect of microstructural anisotropy on mechanical behavior of a high-strength Al–Mg–Si alloy, J. Fail. Anal. Prev. 9 (2009) 114–121.
[48] Y. Estrin, A. Vinogradov, Fatigue behaviour of light alloys with ultrafine grain structure produced by severe plastic deformation: an overview, Int. J. Fatigue 32 (2010) 898–907.
[49] T.-S. Shih, Q.-Y. Chung, Fatigue of as-extruded 7005 aluminum alloy, Mater. Sci. Eng., A 348 (2003) 333–344.